

preceding chapter. Absolute age of the rock from northern part of the area is estimated 119 ± 6 million years by K/Ar method, thus giving the age is in Aptian (upper of the Early Cretaceous). On the other hand, the age of the rock sample taken from southern part of the area near Tabacal River was 64 ± 3.2 million years (early Oligocene). This discrepancy is probably due to the presence of young intrusives along the fault.

Granite is found out at two localities, at the western and southwestern end of the survey area, intruding into the diorite-granodiorite body. Megascopically it is extremely coarse grained. The absolute age is estimated at 106 ± 5 million years (Albian) using the K/Ar method, which coincides with the results of the observation in the field, that identified it younger than the dioritic rocks. Monzonite appears as dykes throughout the area in scale of about several meters to 200m in width and 10m to 4km in length. Quartz porphyry and granite porphyry appear as small dykes in the areas of diorite-granodiorite, granite and their periphery. Andesite appears as small dykes in the whole survey area.

Fault-fissure system in this area could not be identified during the field survey. Based on the airphotograph analysis, significant three lineaments trending NNE-SSW, NE-SW and N-S were extracted at north central and southern parts of the area. Among them, the one at central part seems to be relatively large-scaled fault as it apparently dislocated the Goyllarisquizga Group quartzite about 500 meters vertically, and small discordant outcrop of schist, which would be removed by tectonic movement, are observed near the lineament. The lineament of southeastern part was originally presumed by geological interpretation and every NE-SW faults become unclear in the granodiorite body, that is probably due to the presence of young intrusives which concealed the lineament.

Within the alteration zone, silicified zone and silicified-argillized zone are predominantly distributed in the northern bank and southern bank of Tabacal River, sandwiched between two major fault lines. Surrounding the above alteration zones, a weak argillization and chloritization are spread over the area to form a wide alteration zone. Composition of the minerals of the silicified zone and silicified-argillized zone is simple with abundant quartz and sericite, and minor kaolinite, smectite, jarosite, rutil and anatase.

2) Geochemical survey (Fig. II-19)

Compared with the other semi-detailed survey areas in the average values, a high concentration of zinc (253.18ppm) is observed in this Chontali area. Analyzing the distribution of anomalous zones of each element, it is noted that those of gold, silver, lead and molybdenum are sporadic and very small in scale. Those of zinc and copper appear in a relatively wide area, but low in concentrations.

The detail survey area as a whole belongs to an anomalous area of gold, silver, lead and molybdenum. Analyzing the distribution of geochemical anomalies of each element, it is noted that of gold is large scale overlapping the alteration zones on the northern bank of the Tabacal River as well as small scale overlapping or around the sporadic alteration zones in a small scale. That of silver is small, discontinuous and sporadic. That of lead is also small and discontinuous. Each of

geochemically anomalous zone of silver and lead is found in one locality of semi-detailed survey area. That of zinc is small in scale but continuous, and that of copper and molybdenum is small, discontinuous and sporadic. In the detailed survey area the distribution of anomalous zones for gold, silver, lead, zinc and copper overlap each other, but in semi-detailed survey area they hardly overlap.

3) Gold silver quartz vein

Strike and dip of the quartz veins of the eastern slope of the ridge in west Hualatan is concentrated into the first quadrant in stereographic projection, while that of the southern slope is mainly the first quadrant and subordinately the third quadrants and that of the western slope is equally to the first and third quadrants. As to the northern area number of vein is few and their strike and dip is into the third and fourth quadrant. As a whole, frequency of veins is the most dense in the first quadrant and next in the third quadrant, that means the veins striking NW-SE, dipping south west are most predominant and the vein striking NW-SE, dipping north east is next to the above. (Fig. II-20, 21)

Fig. II-22 shows the average grade of quartz vein of this area. The highest grade is in the quartz vein from west side of Hualatan which is Au:27.3g/t, Ag:17.3g/t. Grade of veins varies in the range of Au:0.41~56.23g/t, Ag:0.7~24.3g/t.

Homogenization temperature of liquid inclusions of quartz vein ranges 92°C to 274°C and average 151°C. Concerning to their distribution, the high temperature of over 200°C tend to distribute near the intrusives and the low temperature of less than 150°C surround the ridge of west Hualatan and the medium temperature of over 150°C is on the top of ridge.

6-2 Geophysical Survey

6-2-1 Electro-magnetic Survey

1. Outline of Survey

Electro-magnetic survey by CSAMT method has been conducted for the surface showings of epithermal mineralization and quartz vein.

Measurement of apparent resistivity was done in the ten different cycles. The results of this and the measurement of resistivity of the rock specimen of typical rock types were used for interpretation, then sections and plan of resistivity distribution were prepared.

2. Results of Analysis

1) Resistivity Profile (Fig. II-24)

The results of one dimensional interpretation give the bottom layer's resistivity is between 500 Ω m and 1,000 Ω m, which assumed as a resistivity basement of the area.

Undulation of the resistivity basement is large in the three sections, A-A', B-B' and C-C'. The basement rise up at the central part of the three sections.

Upheaved parts of the basement are mostly covered with conductive layer under 100 Ω m, even some part being under 50 Ω m. Large discontinuities are appeared on those upheaved parts of the basement resistivity structure. The upheaval of the basement with conductive layer on top and resistivity structure discontinuity are common to the three sections and it is inferred to be a continuous feature for the three sections. Along the section D-D', there is a large upheaval of the basement from Vista Alegre to the intersection with the section B-B', and local upheavals of the basement with resistivity structure discontinuity at the intersection with the section C-C' and north of Tabacal. High resistivity layer is thick and continuous to depths at the center of the section, from the station No. 60 to No. 64. At the stations No. 86 and No. 99, conductive layer is distributed surrounding the upheavals of basement.

2) Resistivity Structure Map (Fig. II-25)

In the resistivity structure map of 1,600 m above sea level, high resistivity zones over 500 Ω m extend N-S direction in the west of Hualatan and are surrounded by conductive zones under 50 Ω m. Major mineralized zones in Chontali area are in these resistive zones extending N-S direction. Conductive zones under 50 Ω m are in the southwest of Vista Alegre. Intruded monzonite and alteration is near the station No. 59, and the conductive zones are assumed to be caused by the intrusion and alteration.

On the resistivity structure map of 1,200 m above sea level a resistive zone of over 500 Ω m is in the southwest of Hualatan which also is seen slightly south of it in the resistivity structure map of 1,600 m above sea level and show upheaval of the basement. A resistive zone of over 500 Ω m is also around Cruz Pampa. There are relatively low resistivity zones of 100 Ω m and between those two resistive zones. A high resistivity zone extends widely from Vista Alegre to Los Laureles in the northwestern part of the survey area. A conductive zone extending from Palo Blanco through Tabacal toward N45° E direction is assumed to reflect extension of an inferred fault in depths.

3) Summary of Analysis

i) A high resistive zone extends to depth in the center to the northwestern part of the survey area. It reaches vertically to the level 1,400 m with corn-shape and outcrops at Cruz Pampa and Hualatan. Interpreting from the relation between this resistive zone and mineralized alteration zone on the surface of the ground, mineralization in Chontali area is closely related to this upheaval of the resistive basement.

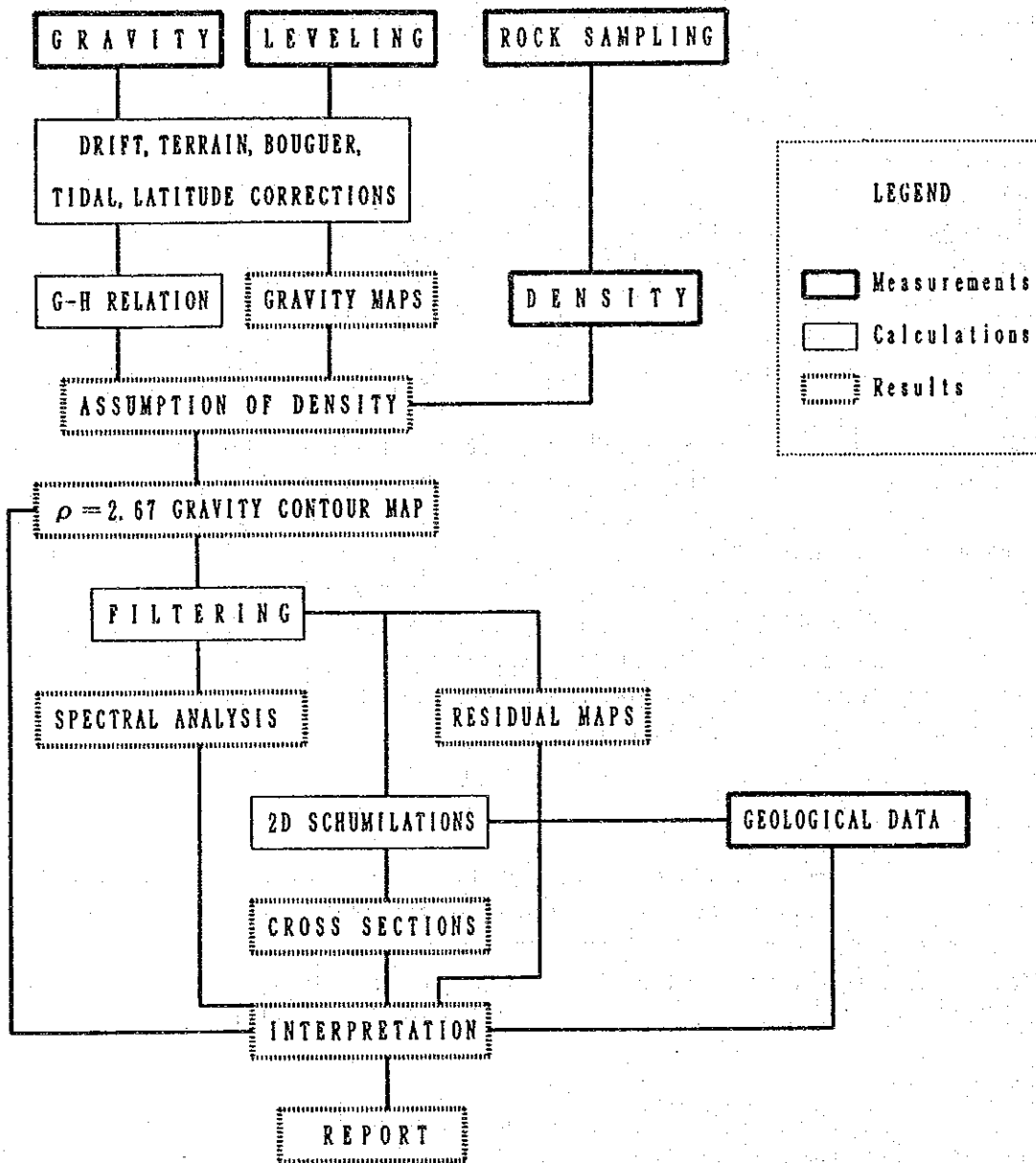
ii) There are conductive zones above and around the upheaval of the resistive basement. Some of them may be due to the effect of alteration zones.

iii) A low to medium resistivity zone extends to depth along the inferred fault through Palo Blanco and Tabacal.

6-2-2 Gravity Survey

1. Outline of Survey

In order to make clear the distribution and underground structure of basement formation and altered rocks, a gravity survey using La Coste gravimeter was conducted. Flow of survey and analysis is given below.



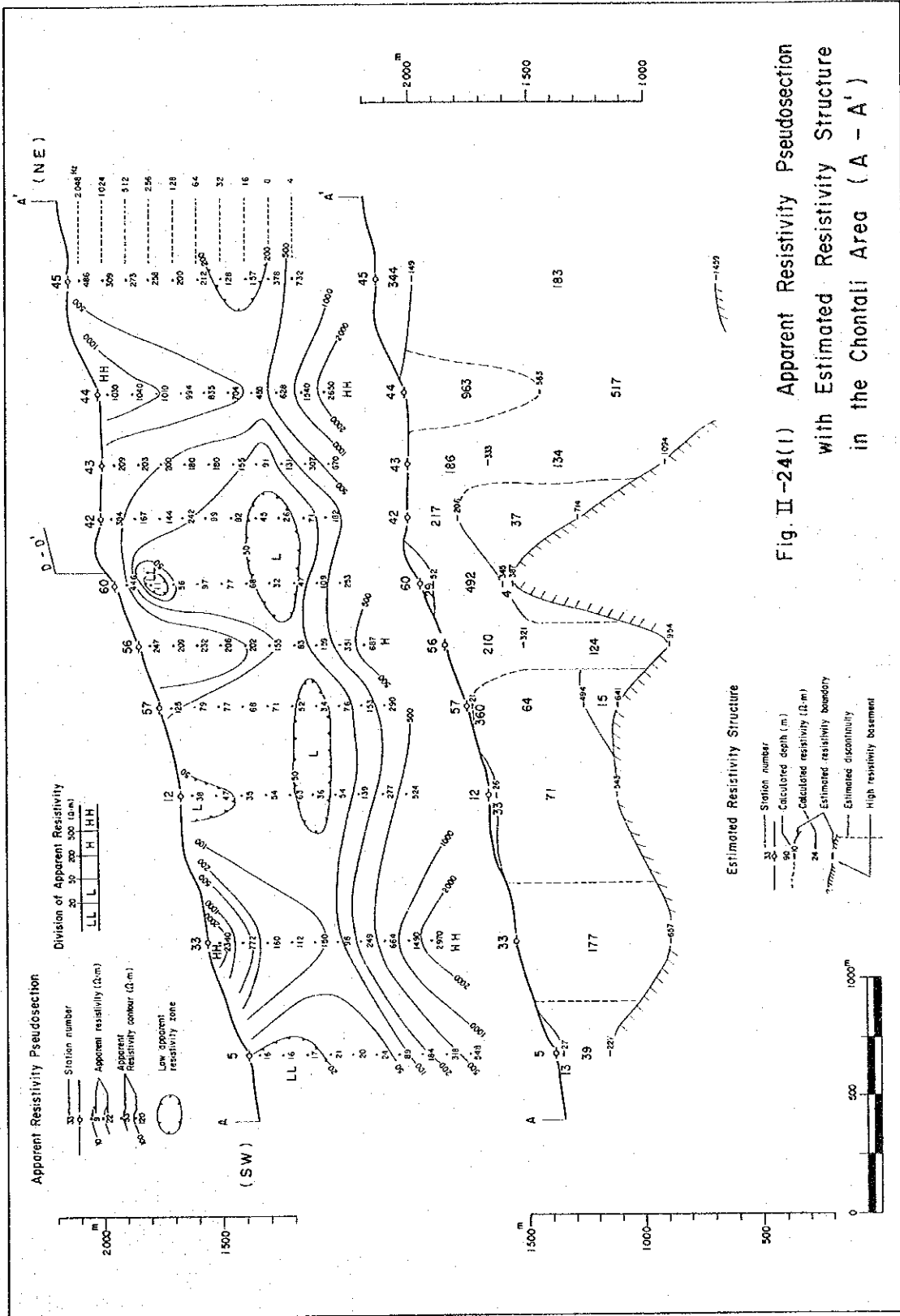
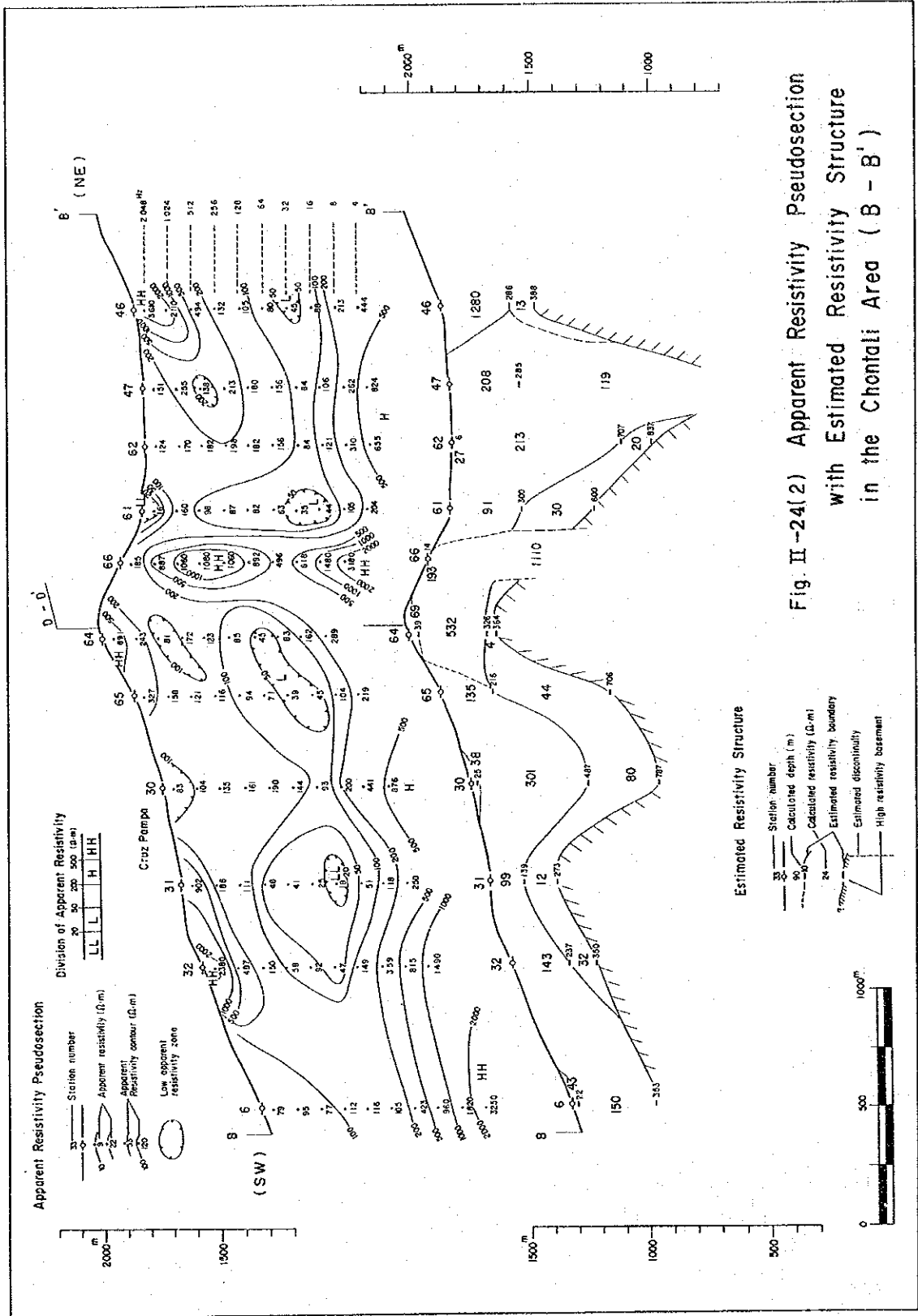
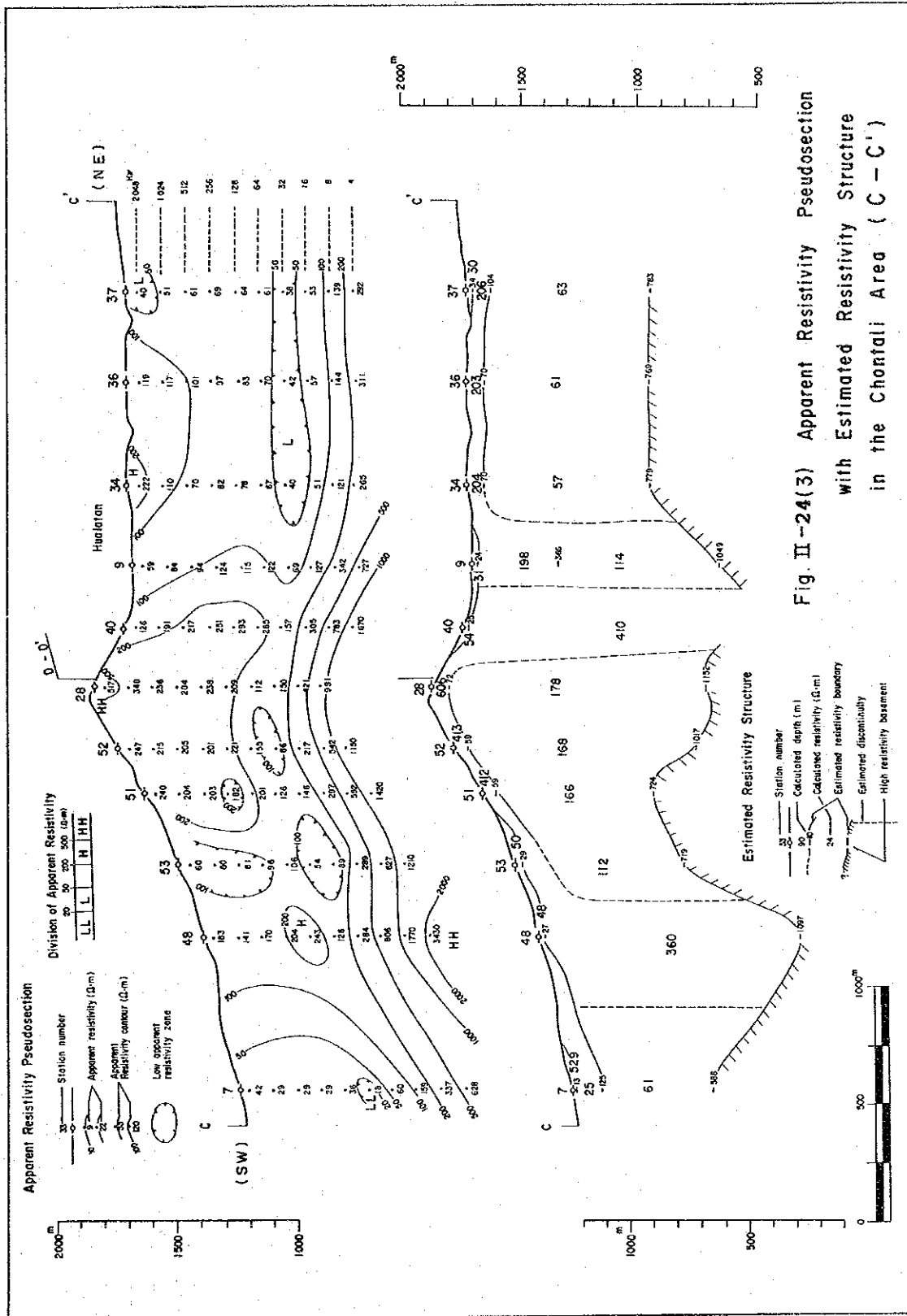


Fig. II-24(1) Apparent Resistivity Pseudosection with Estimated Resistivity Structure in the Chontali Area (A - A')





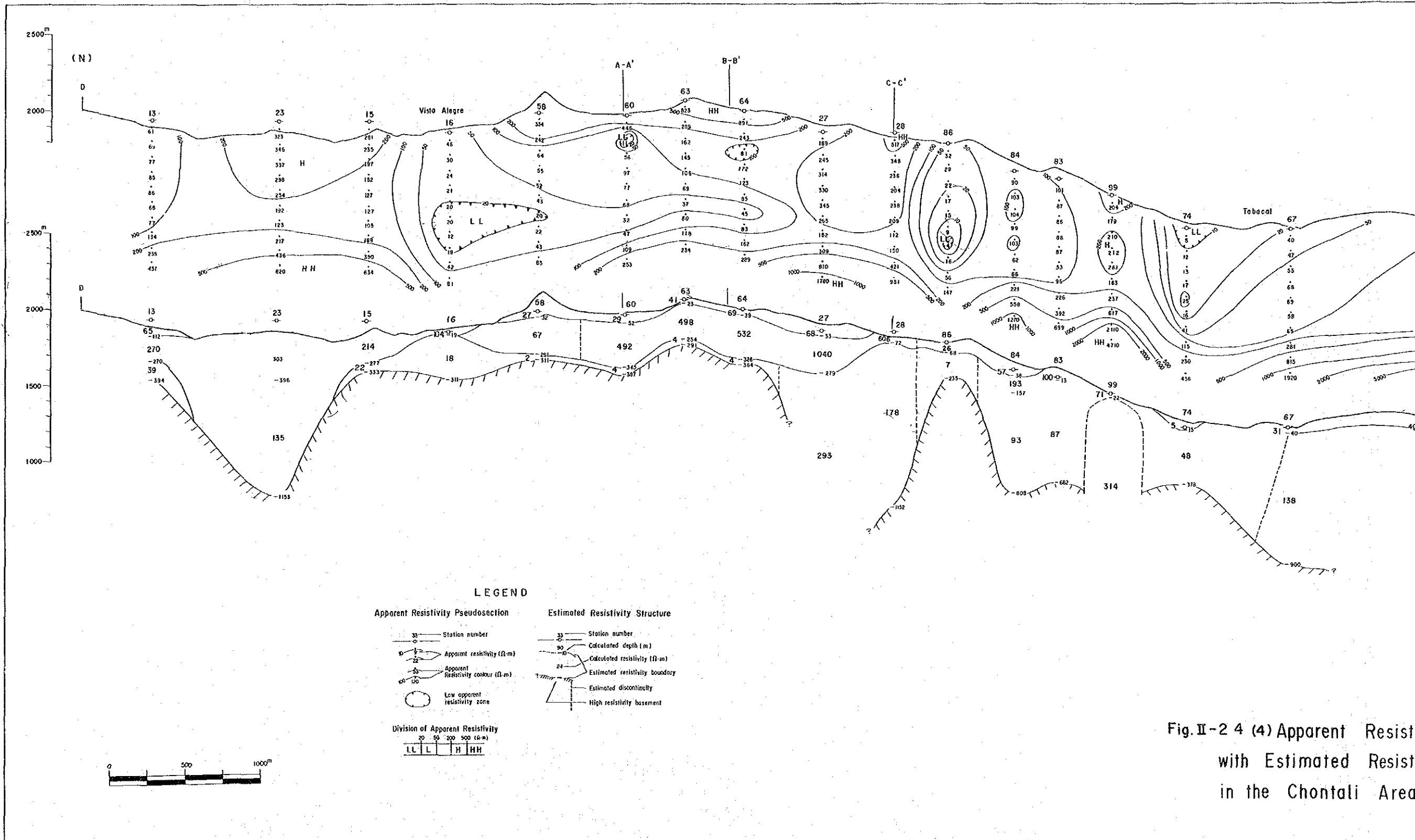
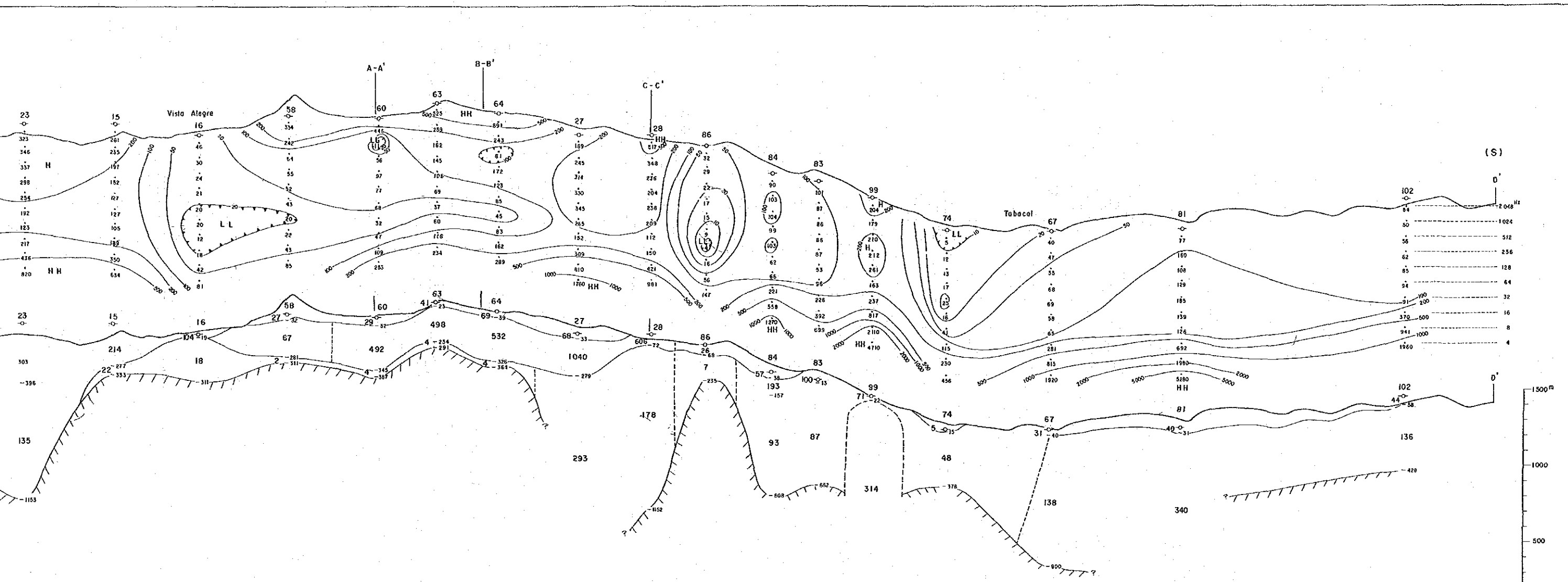


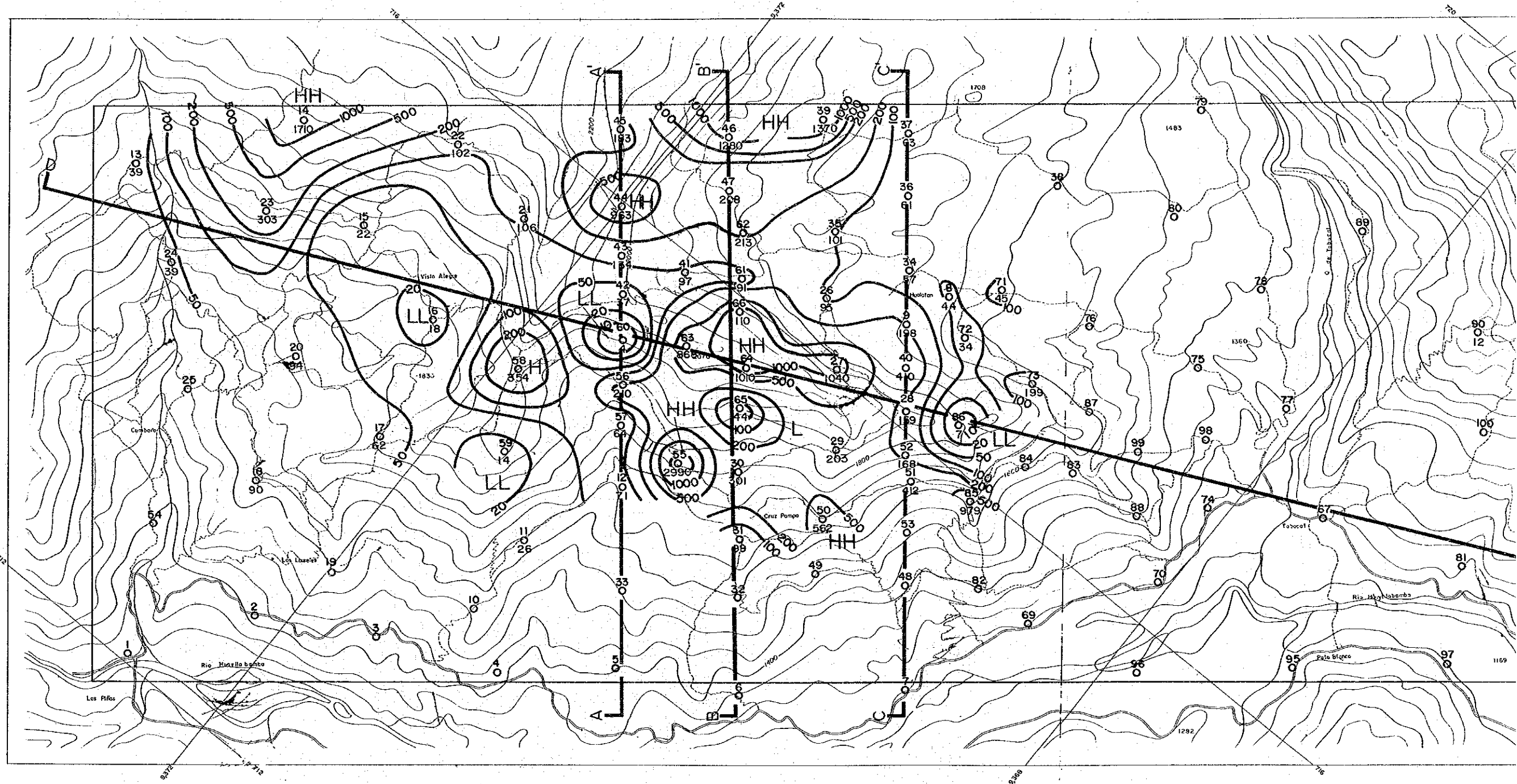
Fig. II-2 4 (4) Apparent Resistivity with Estimated Resistivity in the Chontali Area

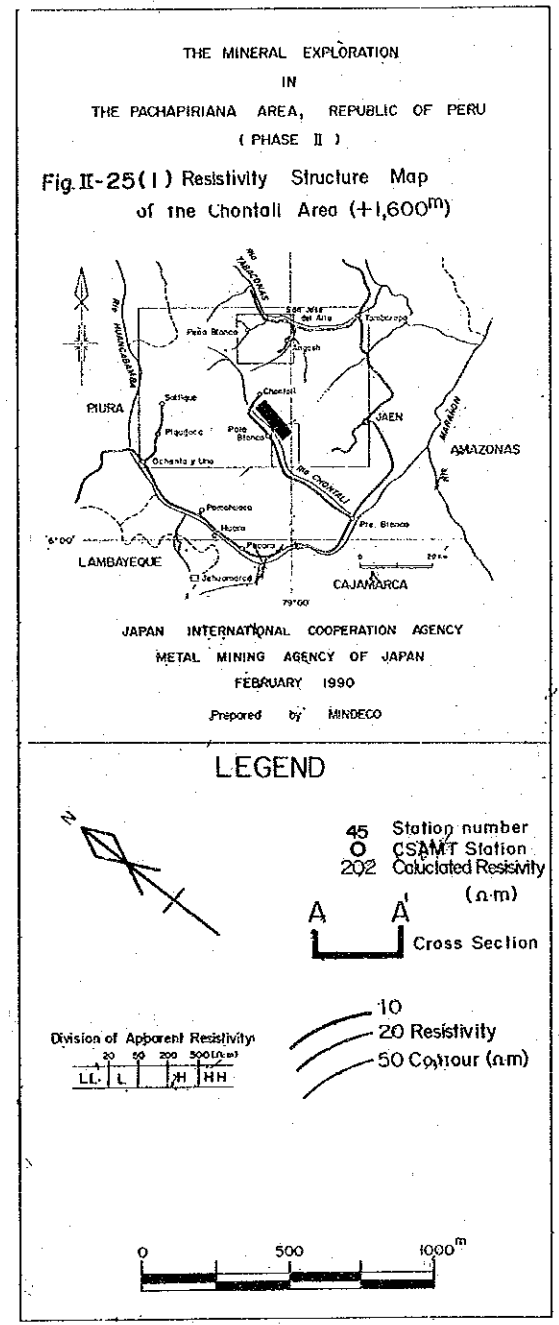
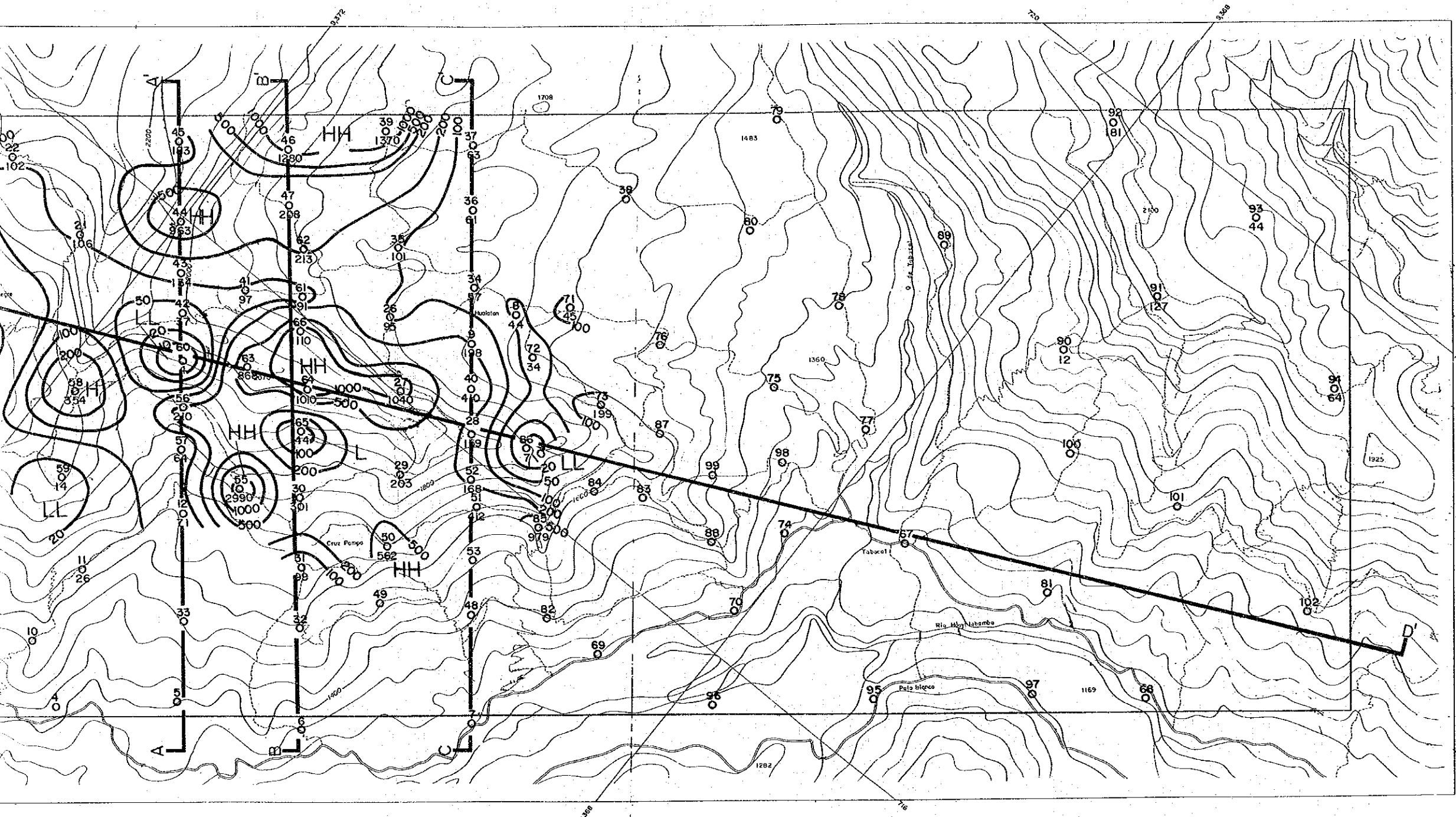


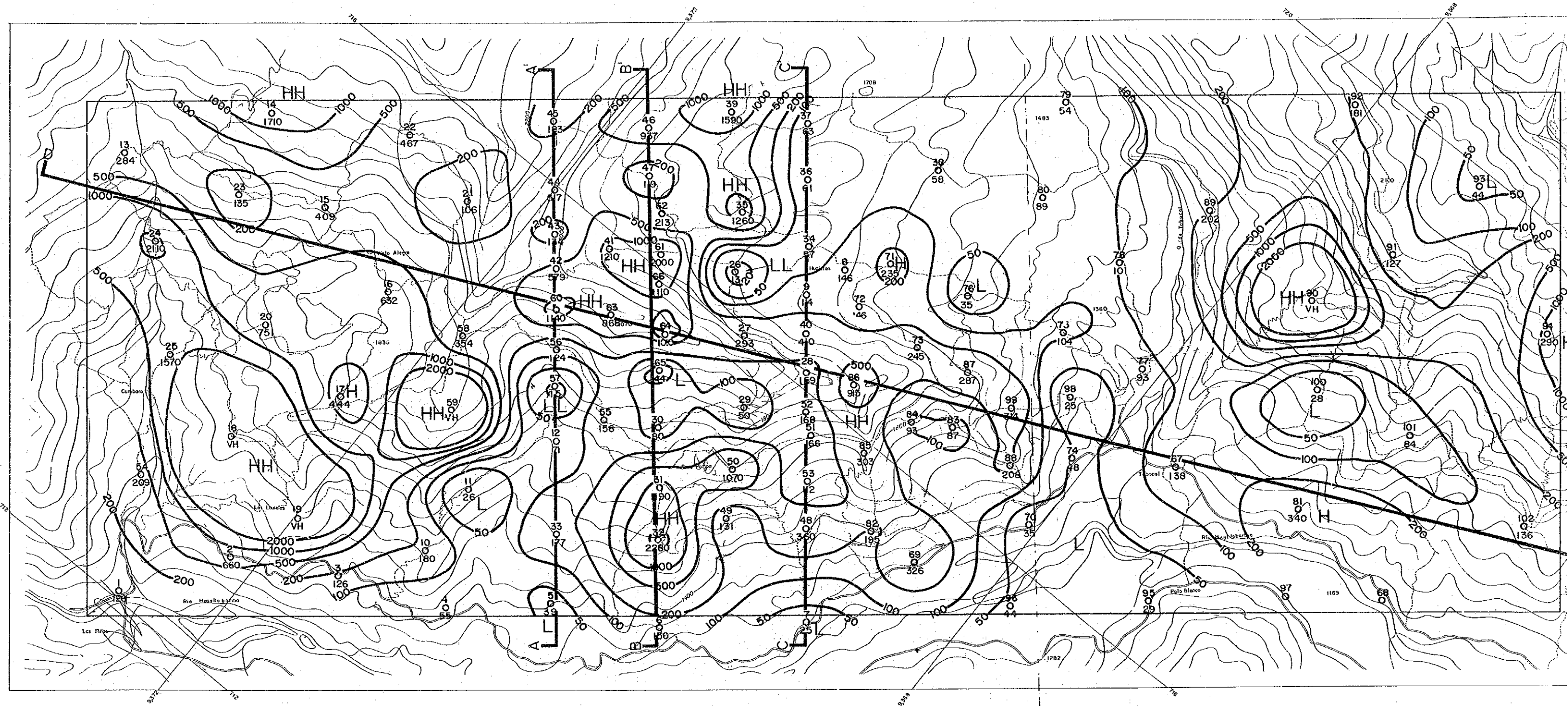
LEGEND

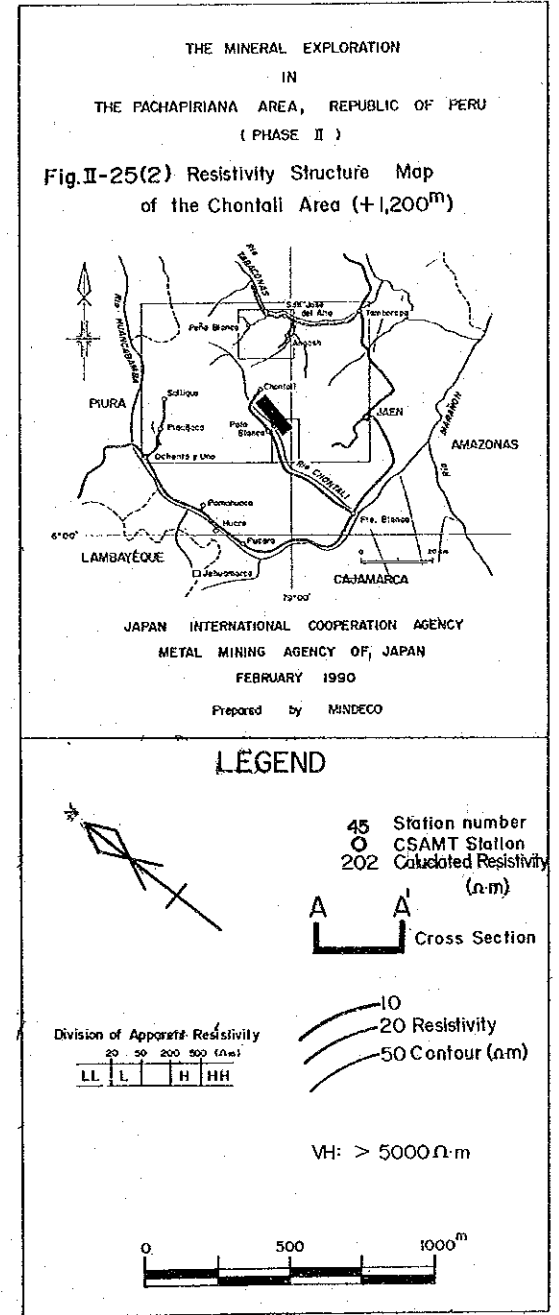
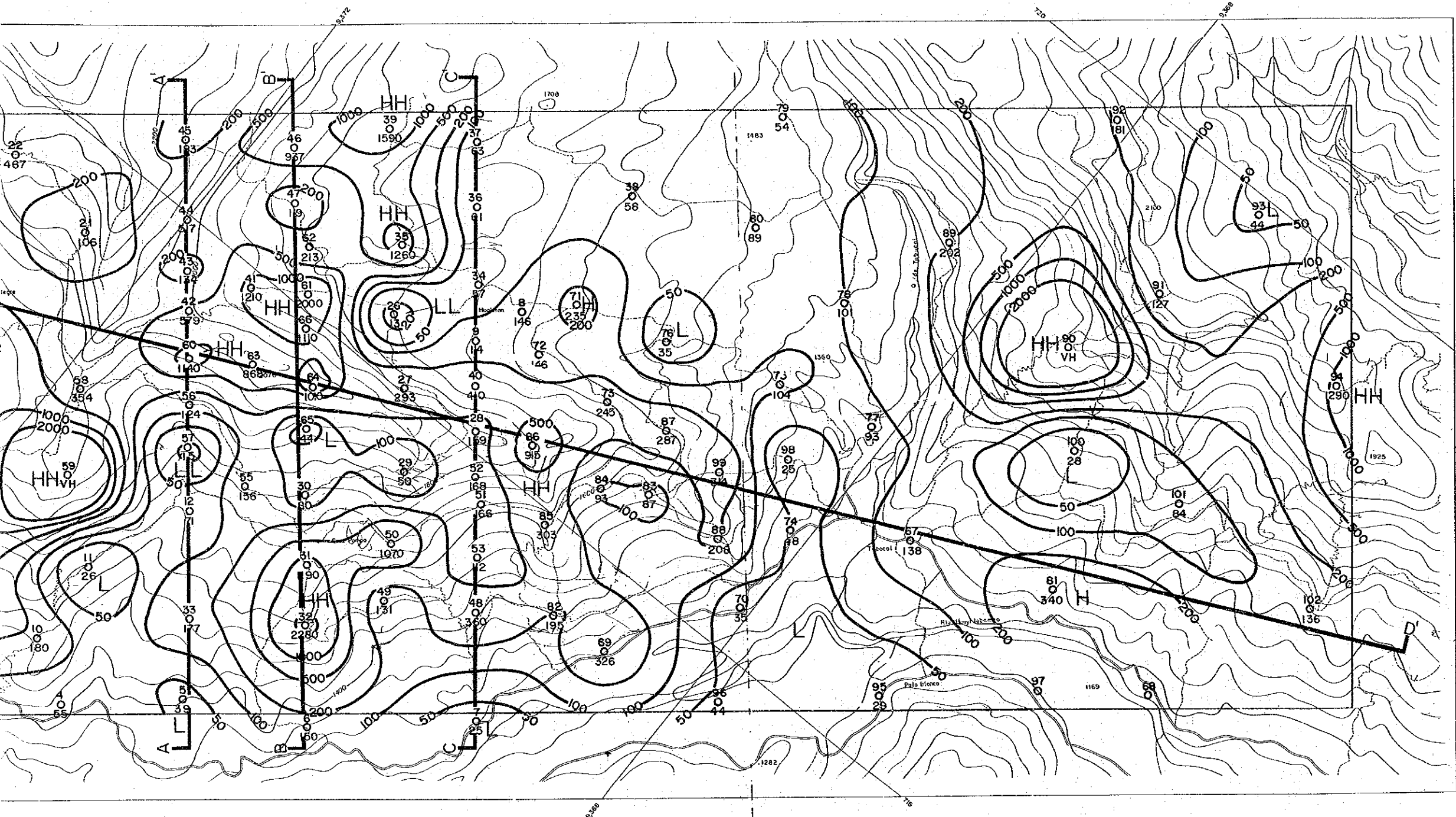
- | Apparent Resistivity Pseudosection | | Estimated Resistivity Structure | |
|------------------------------------|--|---------------------------------|--|
| | Station number | | Station number |
| | Apparent resistivity ($\Omega\cdot m$) | | Calculated depth (m) |
| | Apparent Resistivity contour ($\Omega\cdot m$) | | Calculated resistivity ($\Omega\cdot m$) |
| | Low apparent resistivity zone | | Estimated resistivity boundary |
| | | | Estimated discontinuity |
| | | | High resistivity basement |
-
- | | | | |
|----------------------------------|----|-----|-------------------------|
| Division of Apparent Resistivity | | | |
| 20 | 50 | 200 | 500 ($\Omega\cdot m$) |
| LL | L | H | HH |

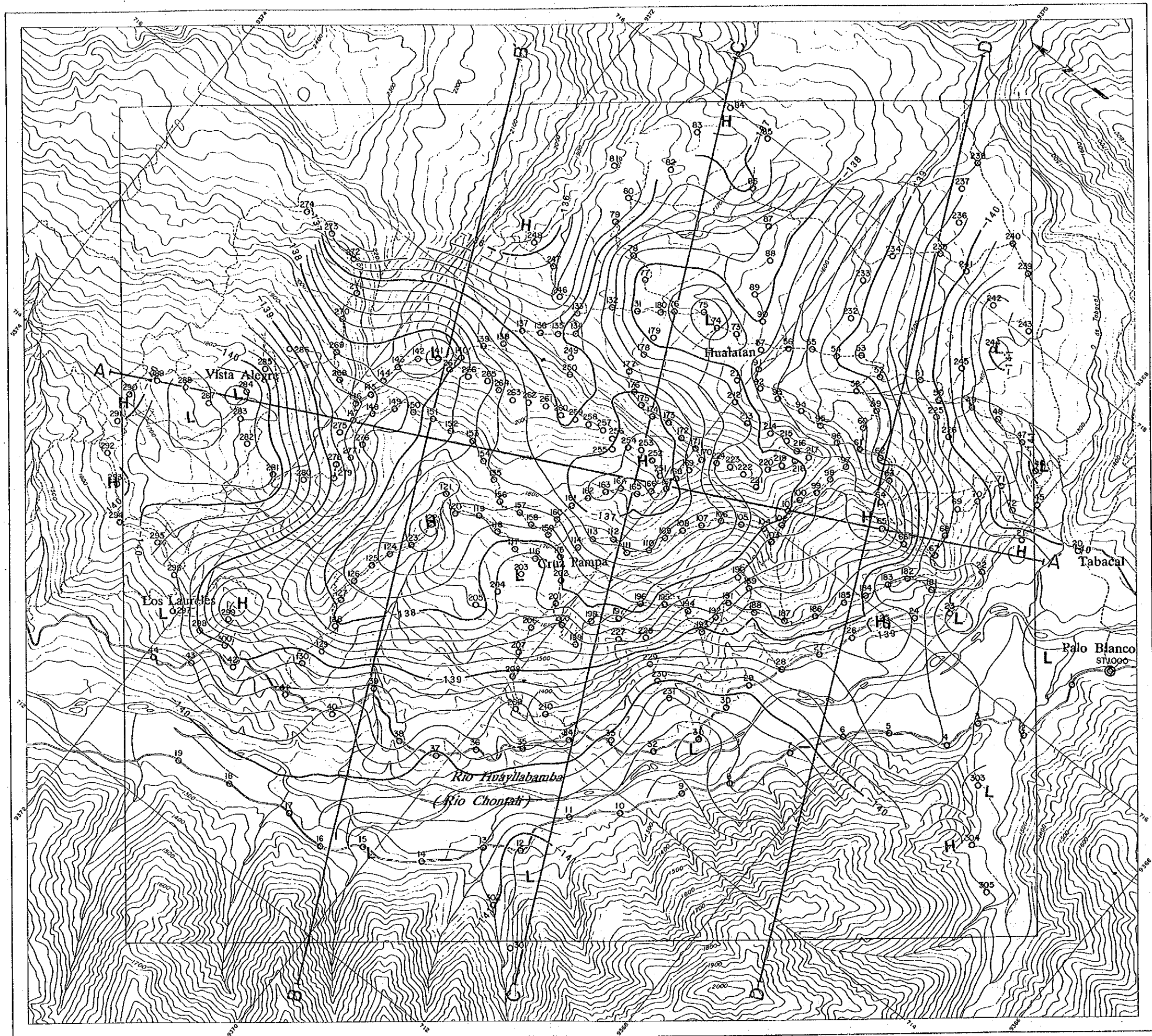
Fig. II-2 4 (4) Apparent Resistivity Pseudosection with Estimated Resistivity Structure in the Chontali Area (D - D')











LEGEND

- O Gravity station
- A-A' Cross section
- 1.0 mgal interval
- - - 0.2 mgal interval
- H High gravity zone
- L Low gravity zone

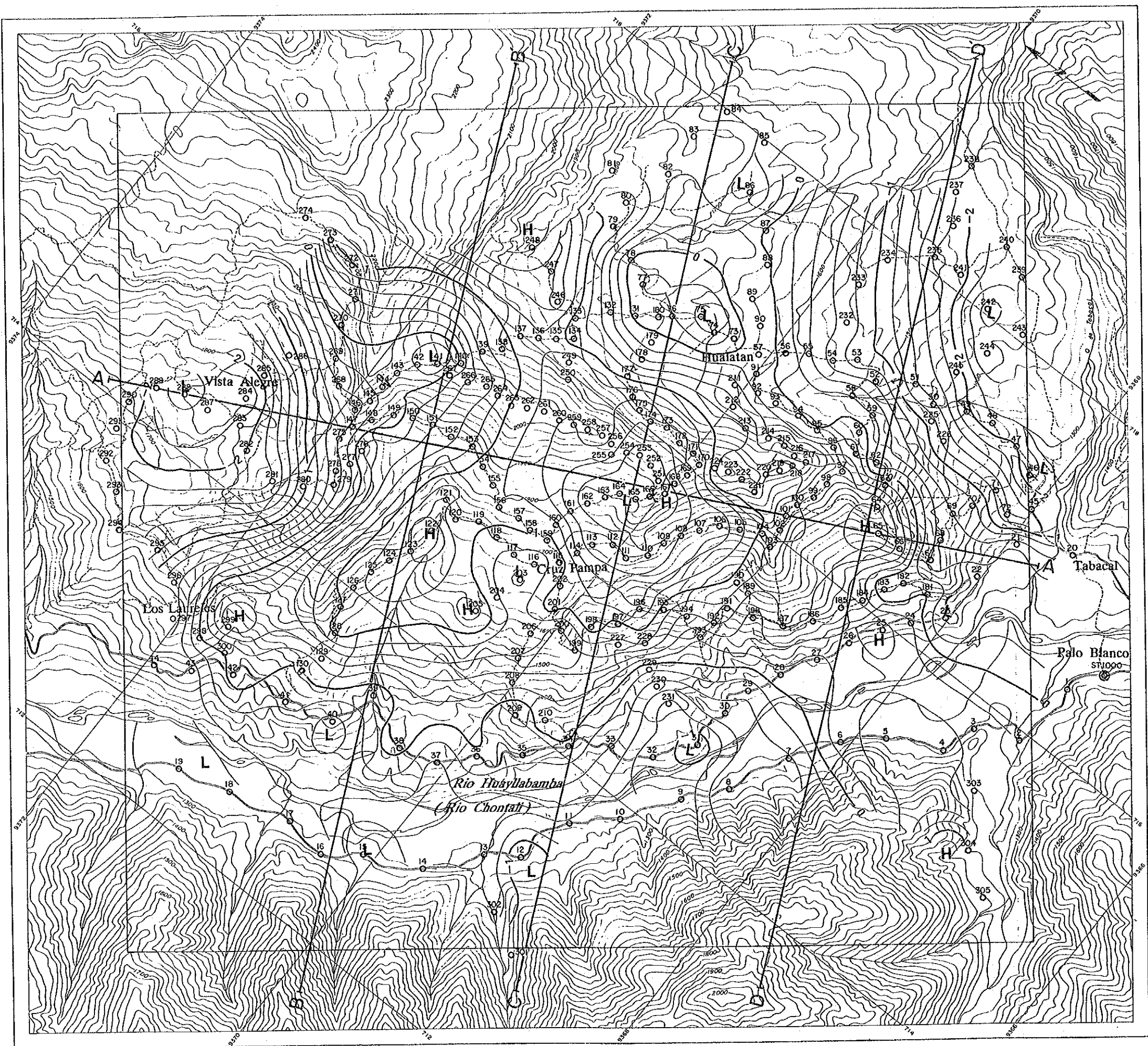
THE MINERAL EXPLORATION
 IN
 THE PACHAPIRIANA AREA
 REPUBLIC OF PERU
 (PHASE III)

GRAVITY SURVEY

Fig. II-26
 Bouguer Anomaly Map
 ($\rho = 2.67 \text{ g/cm}^3$)

FEBRUARY 1991





LEGEND

- O Gravity station
- A-A' Cross section
- 1.0 mgal interval
- - - 0.2 mgal interval
- H High gravity zone
- L Low gravity zone

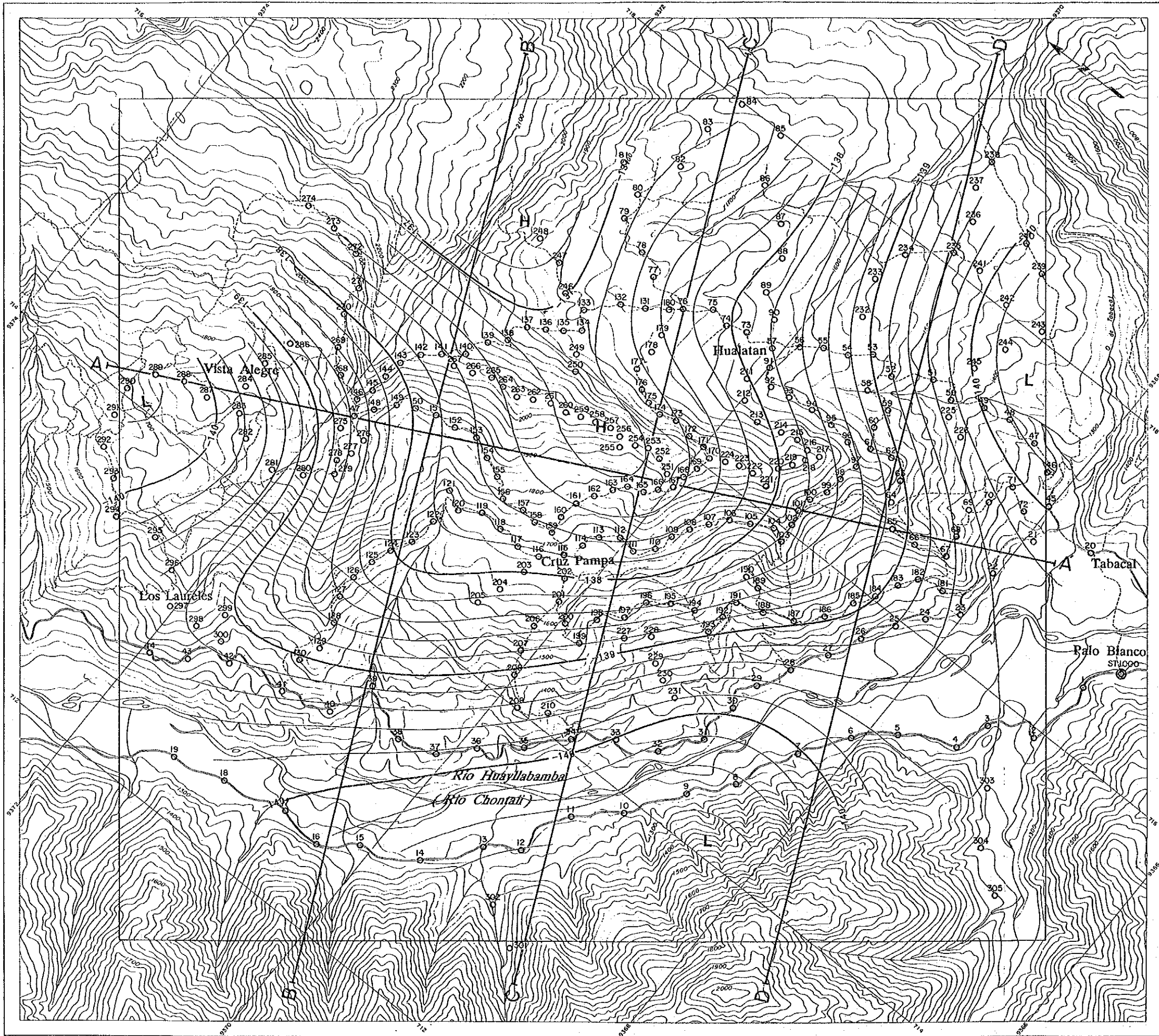
THE MINERAL EXPLORATION
 IN
 THE PACHAPIRIANA AREA
 REPUBLIC OF PERU
 (PHASE III)

GRAVITY SURVEY

Fig. II-27
 First-order
 Residual Gravity
 Map

FEBRUARY 1991





LEGEND

- O Gravity station
- A-A' Cross section
- 1.0 mgal interval
- - - 0.2 mgal interval
- H High gravity zone
- L Low gravity zone

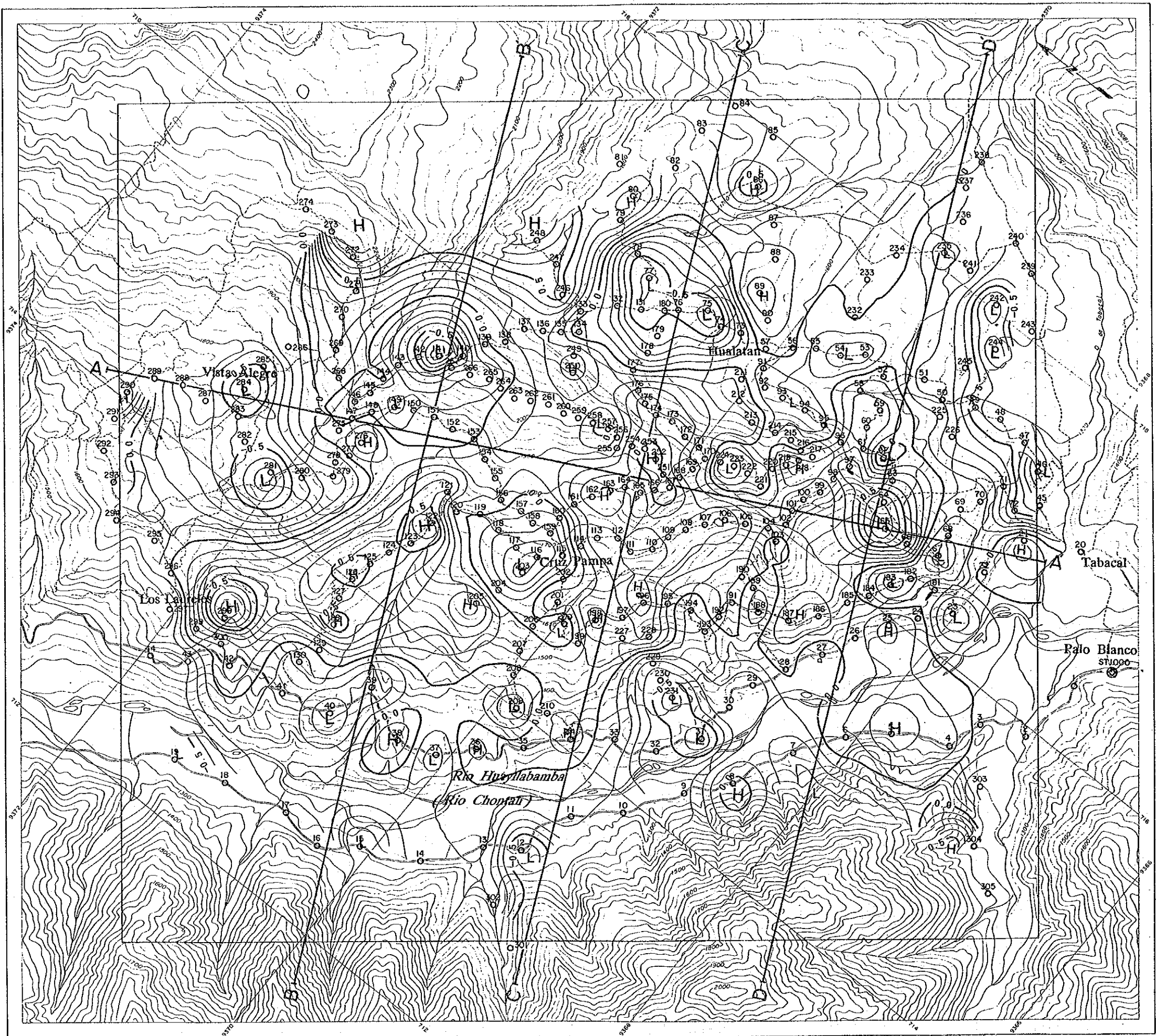
THE MINERAL EXPLORATION
 IN
 THE PACHAPIRIANA AREA
 REPUBLIC OF PERU
 (PHASE III)

GRAVITY SURVEY

Fig. II-28
 Long-wave
 Gravity Map

FEBRUARY 1991





LEGEND

- O Gravity station
- A-A' Cross section
- 0.5 mgal interval
- 0.1 mgal interval
- H High gravity zone
- L Low gravity zone

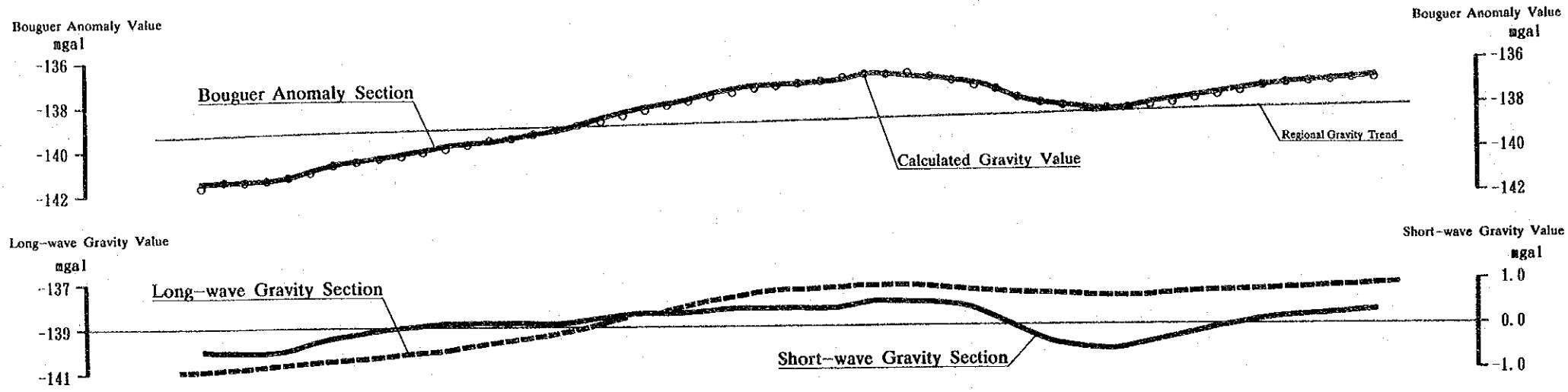
THE MINERAL EXPLORATION
 IN
 THE PACHAPIRIANA AREA
 REPUBLIC OF PERU
 (PHASE III)

GRAVITY SURVEY

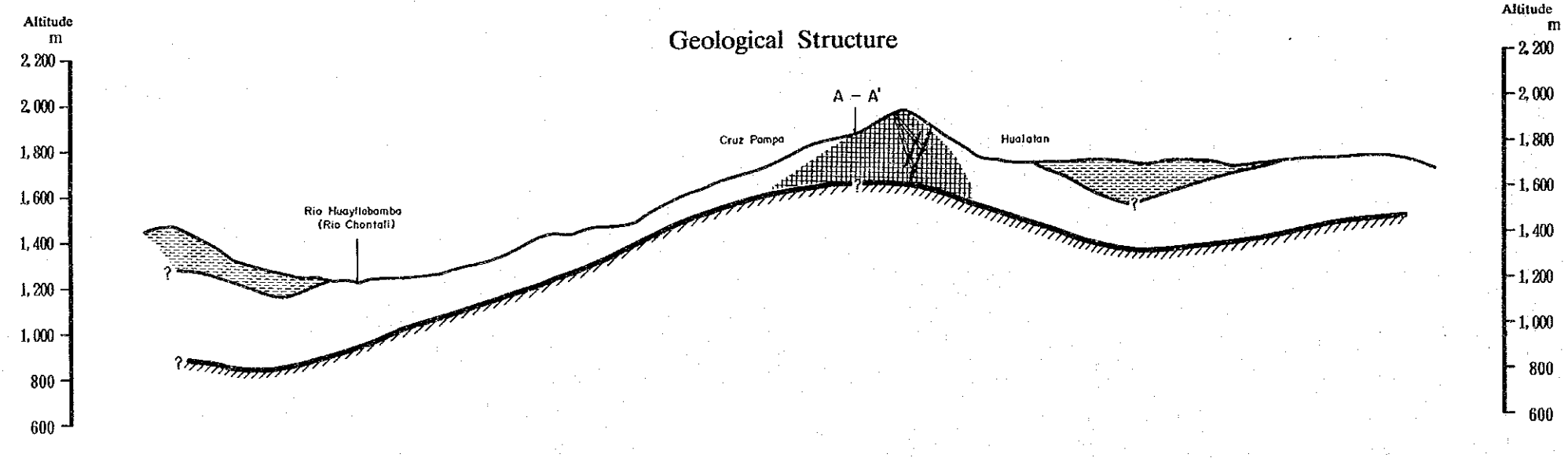
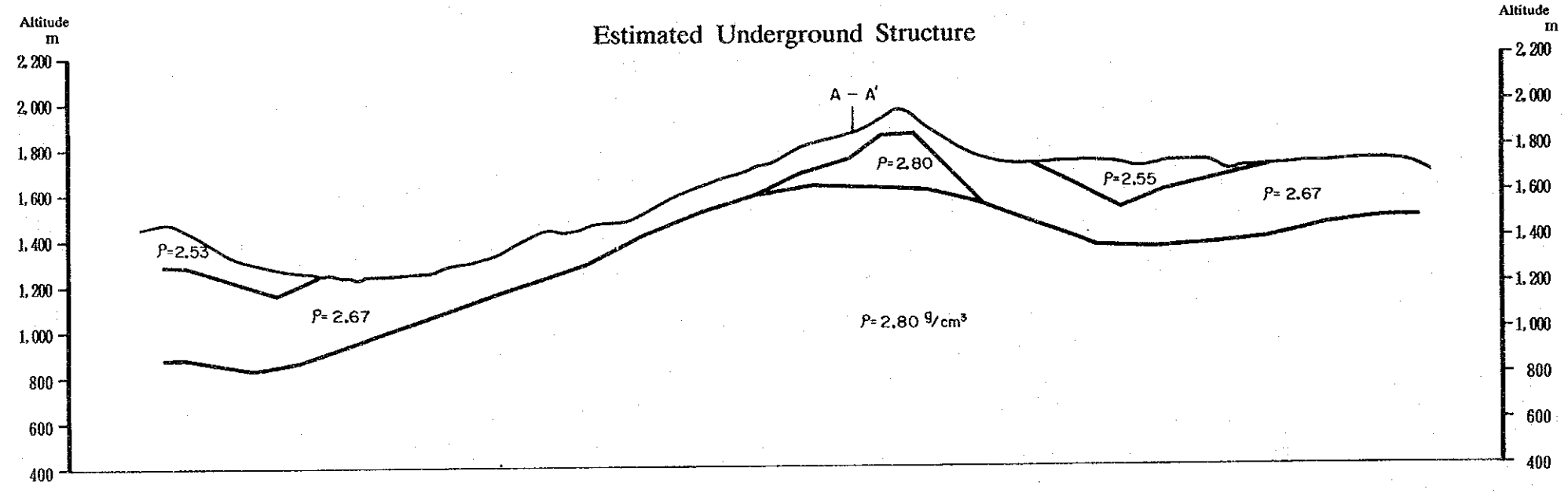
Fig. II-29
 Short-wave
 Gravity Map

FEBRUARY 1991





- LEGEND**
- Boring site
 - Quartz vein
 - Gravity basement
 - High density zone on basement
 - Low density layer



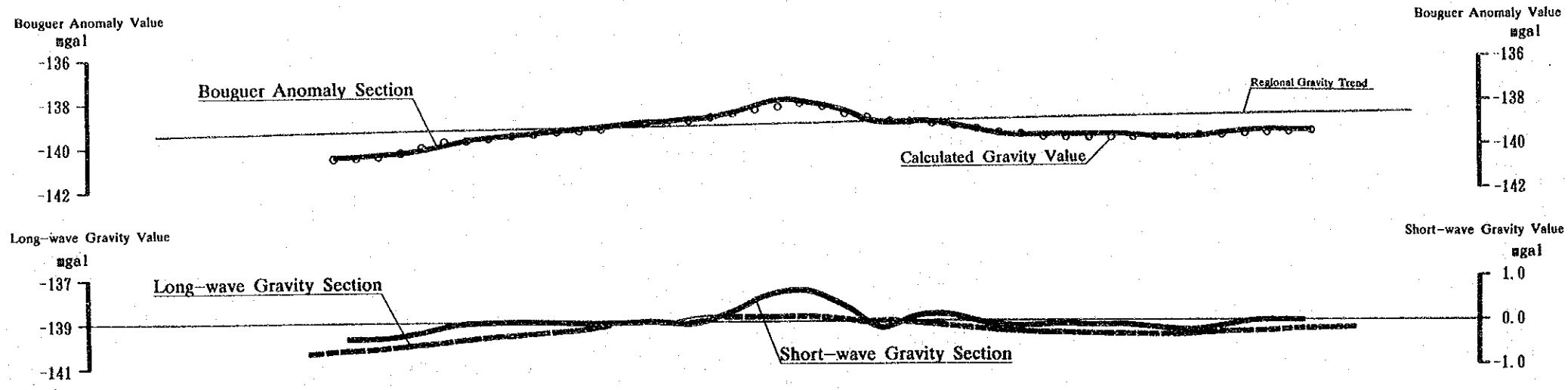
THE MINERAL EXPLORATION
 IN
 THE PACHAPIRIANA AREA
 REPUBLIC OF PERU
 (PHASE III)

GRAVITY SURVEY

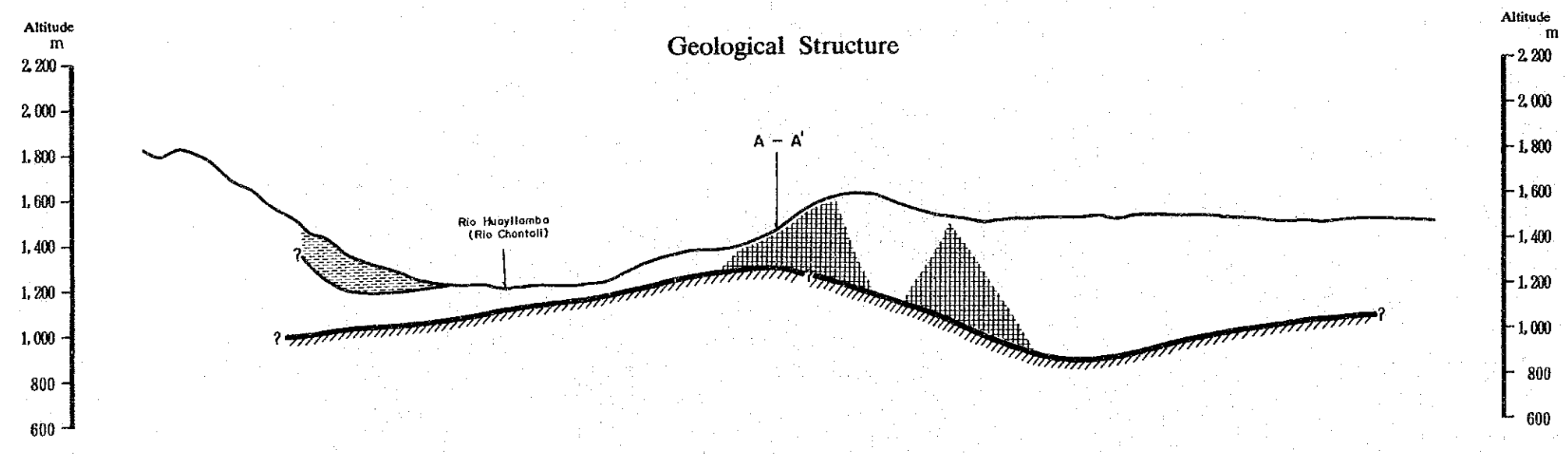
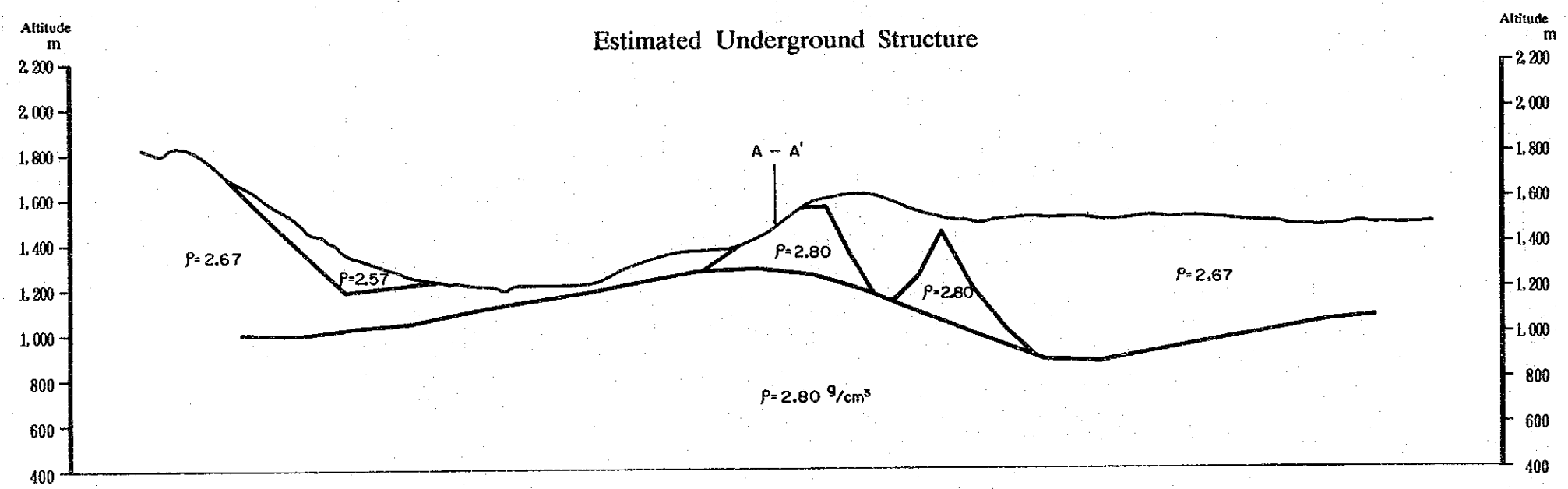
Fig. II-30 (1)
 Cross Section
 of C-C'

FEBRUARY 1991





- LEGEND**
- Gravity basement
 - High density zone on basement
 - Low density layer

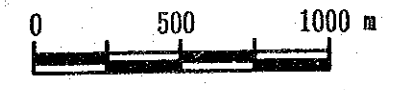


THE MINERAL EXPLORATION
IN
THE PACHAPIRIANA AREA
REPUBLIC OF PERU
(PHASE III)

GRAVITY SURVEY

Fig. II-30 (2)
Cross Section
of D-D'

FEBRUARY 1991



2. Results of Analysis

1) The Bouguer gravity in the survey area is seen to vary from -141 mgal to -138 mgal with a range of only 5 mgal. The maximum gravity gradient is 3 mgal/km near Vista Alegre, eastern survey area (Fig. II-26).

2) Residual gravity values range from -2.4 mgal to 2.0 mgal. High residual gravity anomalies are observed in the center of survey area, surrounded by low residual gravity zones. The gravity high trend NNE-SSW and NW-SE through the center of the survey area (Fig. II-27).

3) In the gravity anomaly of long wave length, a rise of high gravity was detected in central part of the survey area (Fig. II-28).

4) In the gravity anomaly of short wave length, an anomaly of high gravity is seen in the area of gravity rise of long wave length, and the low anomaly is observed in the high anomalies. (Fig. II-29).

5) Analysis of two dimensions simulation showed, there is a two layer structure, with the upper layer (2.68g/cm³), and the lower layer (2.80g/cm³) and locally a low density layer and a high density layer, corresponding to the anomalies of short wave length were detected on the surface and on top of the basement (Fig. II-30).

3. Summary of Results

Underground gravity structure of the area is summarized as follows.

Distribution of the gravity basement is quite similar to the anomaly of long wave length, which forms a gentle dome in the center of the survey area where top of the dome is shallow at 100 meters below the surface. A few small high density bodies are detected near the top of dome structure by interpretation of short wave length map. Similar relation between the dome of the basement and local high density bodies are expected in other area especially in Los Laurens area. Depressions of gravity basement were found in Vista Alegre, in the north, and west bank of Rio Huayllabamba in the south.

6-2-3 Summary of Geophysical Survey Results

Results of electromagnetic survey and gravity survey are briefly summarized as follows.

1. Although the distribution and shape of gravity basement are generally similar to these of resistivity basement, depth of gravity basement is 100 meters shallower than that of resistivity basement.

2. However, there are some discrepancies of resistivity and density of the rocks

between analytical figures (resistivity : over 500 Ω m, density : 2.8g/cm³) and actual measurement of the specimens of granitic rock (resistivity 1,000 Ω m, density 2.68g/cm³)

3. The basement formation forms a gentle dome structure at the central part of the area.

4. Near the center of dome, (western Hualatan and southern Hualatan), existence of a shallow high density body was presumed, that appear to be closely related to the distribution of quartz veins.

5. There is a high resistivity zone in the north of high density body at the center of dome. Swarm of quartz veins occur in the high resistivity zone. A low resistivity zone was detected in the southeast of dome.

6. The dome is thought to be a source of mineralizing solution, and the high resistivity zone above the dome is a potential place for ore deposition.

6-3 Diamond Drilling

6-3-1 Outline of Drilling

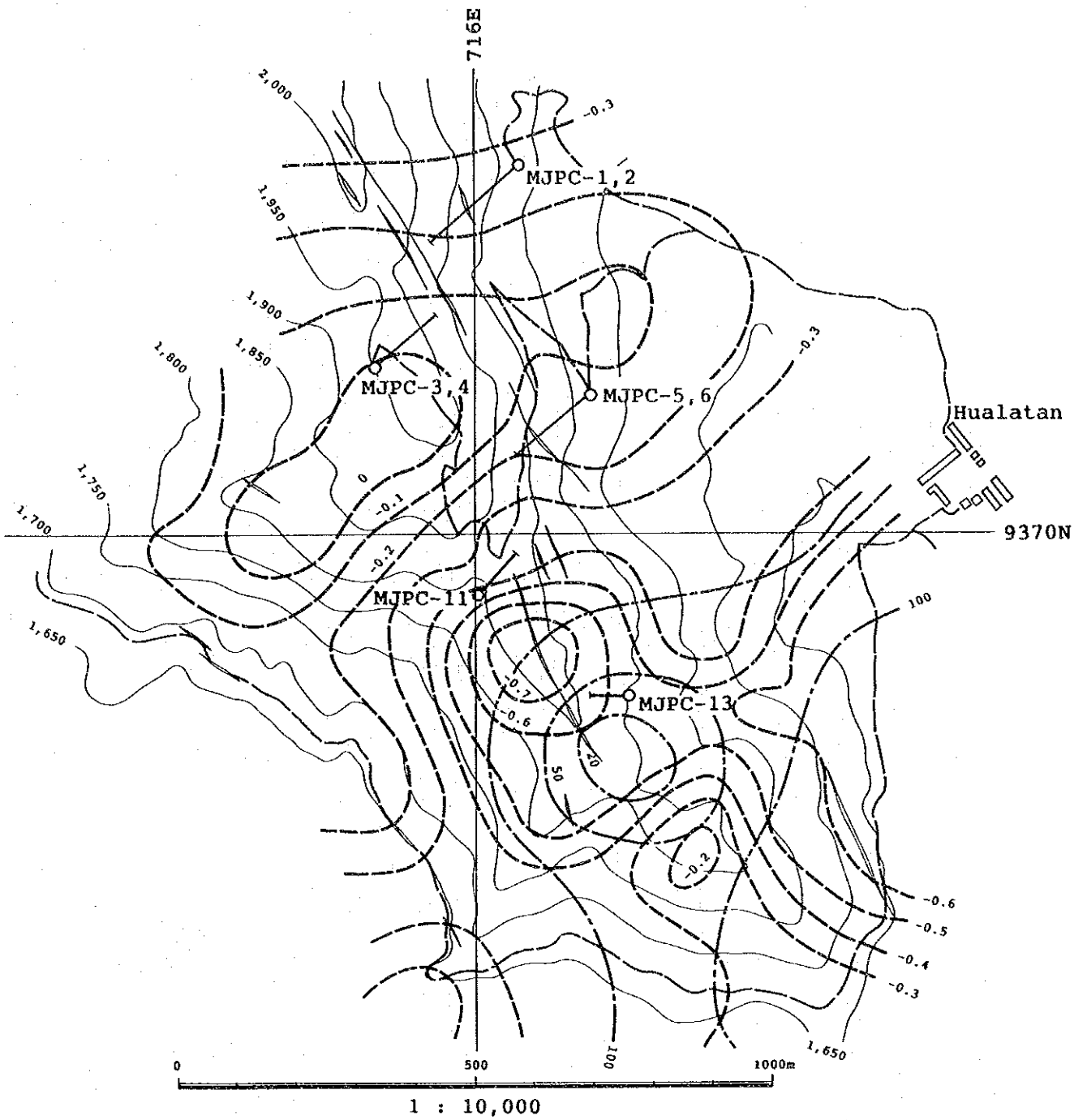
In order to obtain a detail information of the mineralization of quartz veins occur in silicified-argillized zone, vertical panel and then horizontal panel diamond drilling were conducted in the third and fourth years. Diamond drilling was done by Geotec S.A. of Peru under contract basis.

Detail of the drilling is shown in the following table, and the location is shown in Fig. II-31.

Number of Hole	Bearings	Inclination	Length	Coordinate		Elevation
				N	E	
MJPC- 1	230°	-15°	150.00m	9,370,609	716,071	1822.55m
MJPC- 2	230°	-40°	250.00m	9,370,610	716,073	1822.11m
MJPC- 3	50°	-50°	221.16m	9,370,278	715,829	1947.36m
MJPC- 4	50°	-70°	310.00m	9,370,277	715,828	1947.26m
MJPC- 5	230°	-15°	170.50m	9,370,233	716,190	1774.53m
MJPC- 6	230°	-40°	230.85m	9,370,234	716,191	1773.60m
MJPC-11	42°	-50°	145.40m	9,369,898	716,007	1810.00m
MJPC-13	271°	-30°	75.30m	9,369,726	716,257	1848.00m

6-3-2 Results of Drilling

Mineralized zone above Au:1 g/t obtained by diamond drilling is shown in the following table.




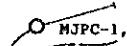
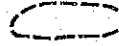
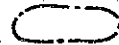
-  Quartz Vein
-  Boring site and Drilling trace and it's number
-  Short wave gravity contour (m gal)
-  256Hz Resistibility contour ($\Omega \cdot m$)

Fig. II - 31 Location of the Drilling with showing Geophysical Survey results in the Chontali Area

Number of Hole	DEPTH		LENGTH	Au g/t	Ag g/t	Remarks	
	m	m					
MJPC- 1	52.45-	52.70	0.25	3.65	11.5	Quartz V	
	102.85-	104.2	1.35	2.05	13.5	Quartz V	
	117.55-	118.65	1.10	1.46	22.0	Quartz V w/Sil-Arg lp tf	
	131.9	-133.3	1.40	2.65	35.0	Quartz V	
	133.9	-134.4	0.50	1.60	5.0	Quartz V	
	146.4	-147.35	0.95	1.05	41.5	Quartz V	
MJPC- 2	149.0	-149.55	0.55	2.50	3.5	Sil-Arg lp tf w/qtz V-let	
	57.95-	58.3	0.35	5.75	4.5	Quartz V	
	59.1	- 61.5	2.40	1.73	7.7	Sil-Arg lp tf w/qtz let	
	100.0	-100.8	0.80	3.20	2.5	Quartz V-let zone	
	116.3	-117.35	1.05	1.05	9.5	Quartz net in breccia zone	
	180.7	-180.90	0.20	1.15	7.0	Quartz breccia	
MJPC- 3	193.5	-194.80	1.30	1.38	38.5	Quartz V	
	43.6	- 43.95	0.35	3.00	2.5	limo Quartz net V	
	44.85-	45.10	0.25	2.40	22.0	wk limo dr-Quartz V	
	63.3	- 64.1	0.80	2.40	22.0	wk limo dr-Quartz V	
	148.75-	151.0	2.25	1.18	24.6	Quartz V w/sil tf br	
	201.6	-202.55	0.95	1.00	6.0	breccia w/Quartz	
MJPC- 4	203.5	-205.5	2.00	2.00	32.3	Quartz V w/breccia	
	206.5	-207.2	0.70	1.70	59.0	Quartz V w/breccia	
	58.9	- 60.35	1.45	1.00	13.5	Sil Arg lp tf	
	MJPC- 5	4.15-	5.35	1.15	1.15	9.5	limo dr-Quartz V
		19.4	- 19.6	0.20	1.05	22.5	Quartz V
		46.8	- 47.05	0.25	1.35	8.0	Quartz V
74.4		- 74.7	0.30	2.30	7.5	dr-Quartz V	
79.85-		80.45	0.60	2.0	25.5	Quartz V	
121.45-	123.75	2.30	1.65	53.5	Quartz V		
MJPC- 6	23.8	- 24.36	0.56	3.45	26.0	Quartz V	
	156.35-	157.05	0.70	1.10	28.5	Quartz V-let	
	158.2	-159.33	1.13	1.70	45.5	Quartz V	
MJPC-11	138.0	-140.15	2.15	no sample	Quartz V		

Mineralization of this area revealed by diamond drilling is briefly summarized as follows:

1. Quartz veins which observed in the surface occur in a wide fractured zone. As the plunge of quartz vein is not vertical, a high grade portion of the vein was not hit right under the high grade portion of the surface.

2. Pyrite is the most predominant mineral. Sphalerite, tetrahedrite, galena and occasional chalcopyrite are frequently observed in quartz vein, quartz veinlets and breccia zones. Native gold was found in MJPC-1 at the depth of 52.6m. Mineral paragenesis of ore shows that the ore minerals except for gold have precipitated simultaneously within a short period, indicating xenothermal type mineralization.

3. Homogenization temperature of liquid inclusions range between 102°C to 194°C, which is higher in the west and lower in the east of the area, suggesting that the granitic rock occurs in the west have played an important role in supplying heat.

4. Carbonitization especially Fe, Mn bearing carbonitization is commonly observed in all drill holes.

6-4 Consideration

Geological structure of this area is not much disturbed. Only two linearments of NE-SW direction were detected by airphoto geological analysis. In Hualatan area sandwiched by this two linearments, an intense silicification and argillization zone have developed and a number of quartz veins were formed in the alteration zone. Mineral assemblage shows that the alteration zone was produced under acidic condition.

A high resistivity body in a gentle dome structure of basement was recognized in the center of alteration zone. Geologically the presence of intrusive intruded into the basement formation consist of granite or diorite~granodiorite is presumed. A similar gentle dome structure of the basement was obtained also in gravity survey. The specific gravity of the basement was interpreted slightly higher than that of granitic rock. This is probably due to the fact that Mn, Fe, Mg-rich carbonitization spread over the basement as observed in drill holes.

Quartz vein occur in a brecciation zone and extension of quartz vein was confirmed up to 200 meters below the surface by diamond drilling. The plunge of the vein is presumed to be steeply dipping southward from the study of fracture pattern and grade of outcrop.

Tetrahedrite, sphalerite, galena, chalcopyrite and native gold was identified as ore minerals. Mineral paragenesis shows the above ore minerals except for native gold have been precipitated simultaneously in a short period, indicating xenothermal type mineralization.

Homogenization temperature of liquid inclusions is low, which range 92~274°C, average 151°C in the surface and 102~194°C, average 137°C in drill holes. Since the optimum temperature of gold deposition is 180~230°C, it is possible that the higher grade of gold mineralization may exist in the depth.

Assuming the high density body delineated by short wave length gravity anomaly was formed by carbonitization of alkaline condition, such high density body might have been formed by the residual solution after gold deposition which is closely related with acidic condition.

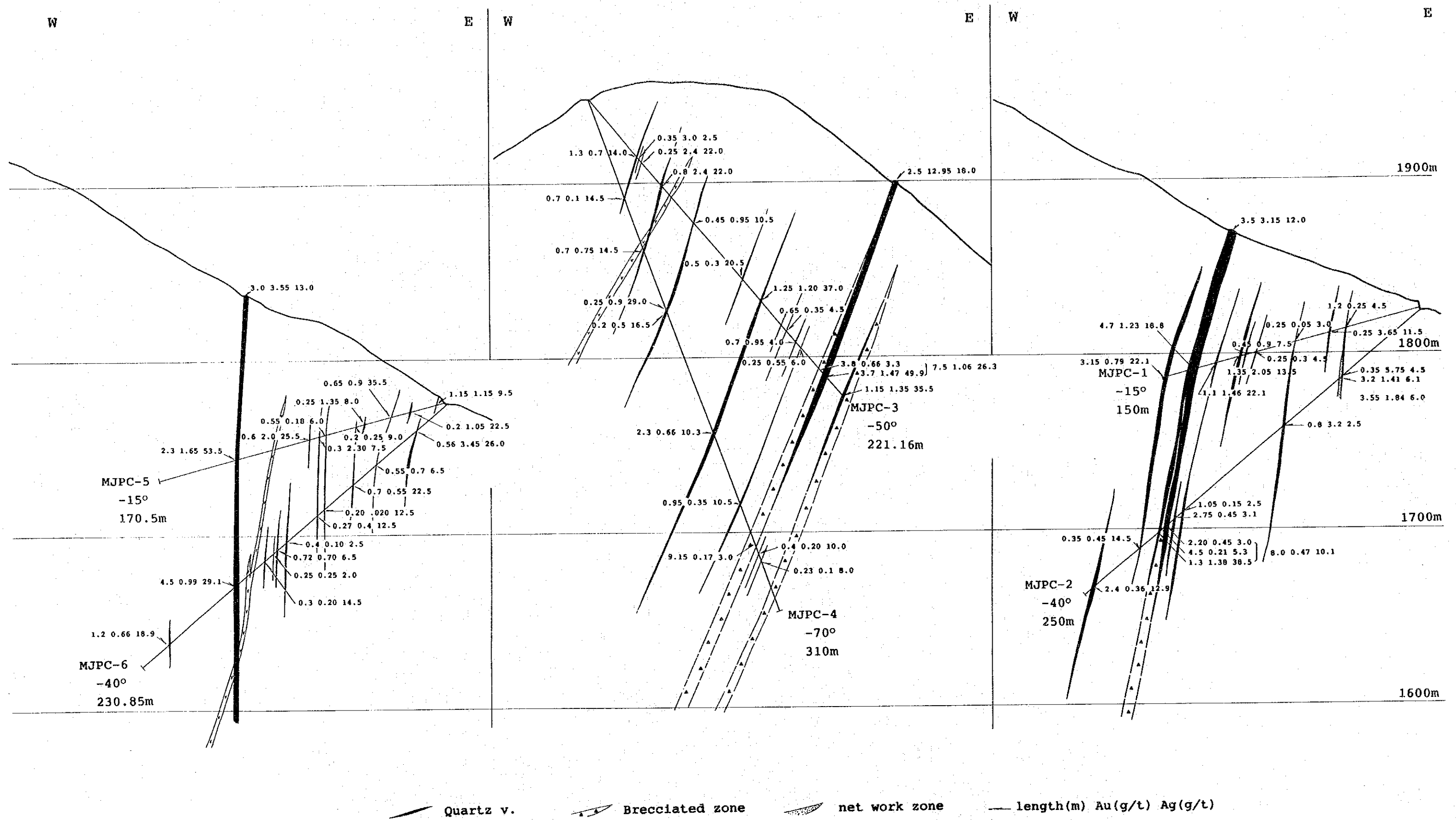


Fig. II -32 (1)

Assay Results on the Profiles of the Drillings in the Chontali Area

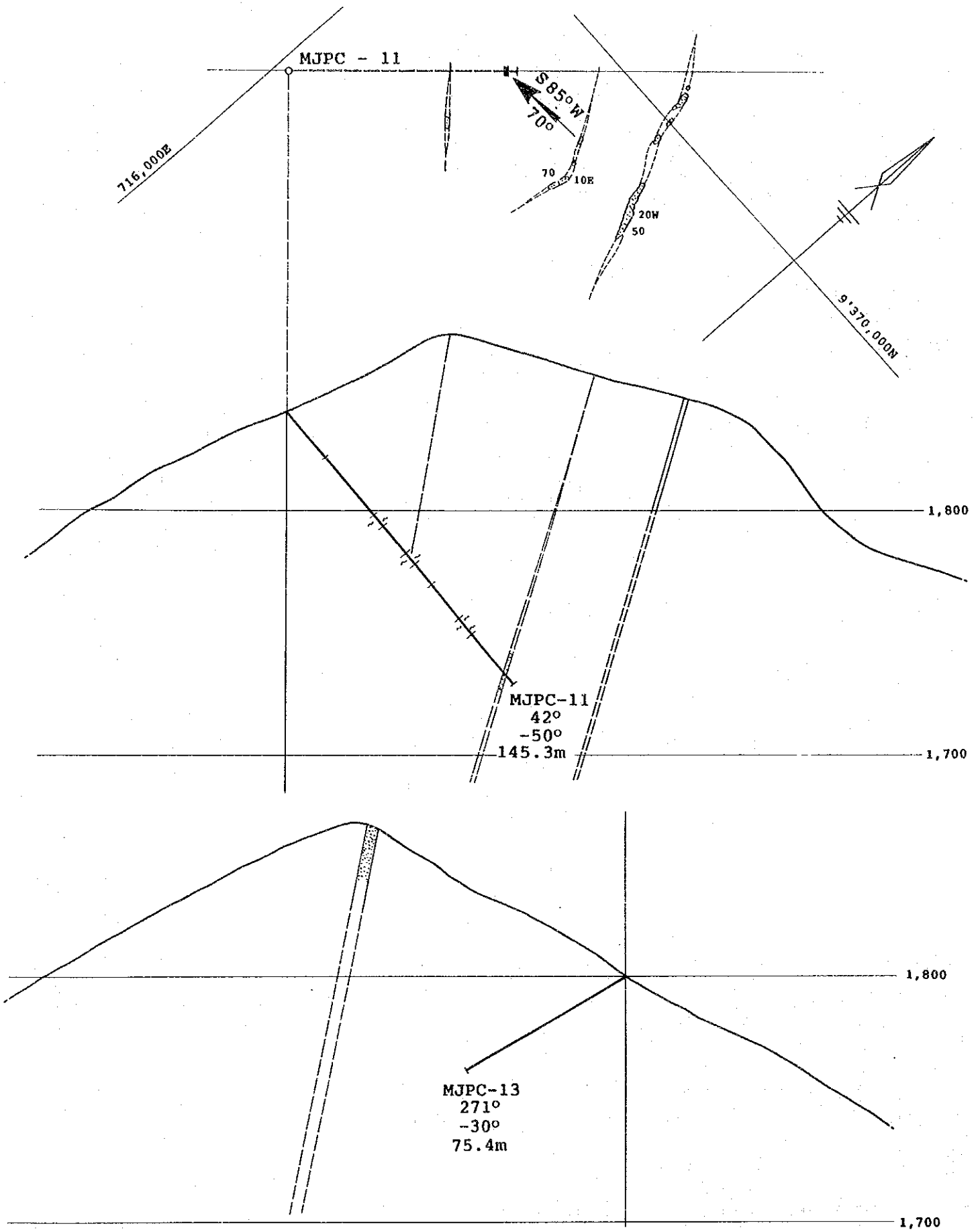


Fig. II-32 (2)

Generalized Profiles of the Drillings in the Chontali Area

Part III CONCLUSION AND RECOMMENDATION

Chapter 1 CONCLUSION

Mineralized host rocks of the survey area are confined to the certain formations such as Leche Limestone, Oyotun Volcanics and Porculla Volcanics. Mineralization showings within Oyotun Volcanics were observed in four areas among the five surveyed areas, while mineralization showing within Leche Limestone and Porculla Volcanics occur in one area among the five.

The showings of mineralization in Oyotun Volcanics can be classified into porphyry copper type, skarn type and epithermal vein type. The showings of porphyry copper type occur at La Huaca of San Felipe area and Zonanga of Palma area. The showings of skarn type mineralization are distributed in Paramo of San Felipe area and Miraflores Sur of Palma area. The showings of epithermal vein type are distributed in Pena Verde of San Felipe area and Hualatan of Chontali area.

The showings in Oyotun Volcanics are the type of epithermal dissemination or vein and found out in Jehuamarca area. The showings in Leche Limestone is skarn type distributed in Angash of Pena Blanca area.

The porphyry copper type showing of La Huaca was surveyed by electro-magnetic survey and a large low resistivity zone was found out. The showings of skarn type are too small and low grade to be workable deposits.

The showings of epithermal dissemination or vein types are surveyed by electro-magnetic survey and distribution of resistivity became clear in every showings. In Pena Verde a small low resistivity body was found near the silicified rock. In Hualatan, a gentle dome of resistivity basement surrounded by wide spread of low resistivity area that indicate an intrusive body was recognized. In Jehuamarca, a high resistivity body in low resistivity background, indicating a silicification zone was found out. Gravity survey was conducted in Hualatan, and obtained a similar basement structure to that of resistivity. Beside a high density body on the gentle dome structure of basement which suggest the presence of mineralization was found out.

Diamond drilling was carried out in Jehuamarca and Hualatan. In Jehuamarca, a dissemination zone of copper, zinc, lead, gold and silver associated with silicification was found out. However, the grade of the deposit is too low to be economical at present metal price. Thus this is to be taken into account as a future resources.

In Hualatan, gold mineralization in quartz vein was detected. The plunge of mineralized zone is presumed to be steeply dipping toward south from the fracture pattern and grade of outcrop. Homogenization temperature of liquid inclusion of vein quartz of Hualatan is 151°C in average which is much lower than the optimum temperature of gold mineralization. So, a higher grade portion can be expected in the depth.

Chapter 2 RECOMMENDATION

1. Geophysical survey by SIP method to determine the sulphide deposits is recommendable to the porphyry copper type mineralization in La Huaca of San Felipe area, where a large low resistivity zone was detected by electro-magnetic survey. In Zonanga of Palma area, to make clear the geological structure and distribution of resistivity, electro-magnetic survey as CSAMT method is recommendable to be carried out.

2. Hualatan of Chontali area is the most potential area for gold deposits. Application of following survey methods is recommendable for further exploration.

1) Detailed mapping and sampling of outcrops

To make clear a structural pattern of the vein in outcrop which control plunge and grade of mineralized zone, a detail mapping (scale 1/500) and detail sampling (every 2-5m) are required.

2) Horizontal panel drilling

To determine the plunge of vein, at least three drill hole, one at the center of presumed plunge and two in the both side of plunge are required.

3) Vertical panel drilling

To find out the vertical extension and potential of mineralization, vertical panel drilling is to be done to the extension of plunge determined by the horizontal panel drilling.

REFERENCES

1. Bellido B., E. (1969)
Sinopsis de la Geologia del Peru.
INGEMMET, Vol.22, Serie A.
2. BRGM (1977)
Informe sobre los resultados de la prospeccion del indicio del tipo de porfide del cobre de la Huaca, Phase 1.
3. Cobbing, J. (1973)
Geologia de los Cuadrangulos de Barranca, Ambar, Oyon, Huacho, Huaral y Canta.
Servicio de Geologia y Minería, Bol. No.26.
4. Cobbing, E.J., Pitcher, W. S., Wilson, J.J., Baldok, J.W., Talor, W.P., MacCourt, W. and Snelling, N.J. (1981)
The geology of the Western Cordillera of Northern Peru.
Institute of Geological sciences overseas memoir 5, London.
5. Davila M., D. and De la Crus B., N.
Geologia del cuadrangulo de Jaen.
INGEMMET(inedited)
6. Davila M., D. and La Torre V., O.
Geologia del cuadrangulo de San Ignacio.
INGEMMET(inedited)
7. Flores N., G. (1972)
Estudio geologico-geoquimico de la anomalia A-4 de La Vega.
INGEMMET(inedited)
8. Flores, G. (1982)
Exploracion y geologia del yacimiento La Granja.
XVI Convencion de ingenieros de minas.
9. Flores, G. and Jimenez, C. (1977)
Informe geologico preliminar del prospecto Jehuamrca, Lambayque.
INGEMMET(inedited)
10. Flores, G., Zelaya, A. and Mamani, F. (1974)
Geologia del deposito de cobre diseminado La Huaca.
INGEMMET(inedited)
11. Flores, G., Zelaya, A., Maya, T. and Mamani, F.
Geologia del deposito de cobre diseminado "Canariaco".
INGEMMET(inedited)
12. Hiroshima, T. et al (1978)
Gravity Terrain Corrections using Graphic Display.
SEG Japan Vol.31-5, p.29-39. (in Japanese)
13. Mamani, F. and Jimenes, C. (1976)
Estudio geologico preliminar del area anomalia el Paramo.
INGEMMET(inedited)

14. Mamani, F. and Moya, L., T. (1974)
Geologia del prospecto Pena Verde.
INGEMMET (inedited)
15. Mamani, F., Agramonte, J., Zegarra, J., Quispe, L. and Galloso, A. (1986)
Proyecto Integral Chinchipe-Cordiera del Condor; Informe de Avances.
INGEMMET (inedited)
16. Mamani, F., Jimenes, C., Sanchez, W., Zegarra, J. and Quispe, L. (1987)
Proyecto Integral Chinchipe; Informe de Avances.
INGEMMET (inedited)
17. Ponzoni S., E. (1980)
Metalogenia del Peru.
INGEMMET
18. Reyes, L. and Caldas, J. (1987)
Geologia de los cuadrangulos de La Playas, La Tina, Las Lomas, Ayabaca,
San Antonio, Chalicanas, Morropon, Huancabamba, Olmos y Pomahuaca.
INGEMMET, Serie A. Vol.39.
19. Shepherd, G.L. and Moberly, R. (1981)
Coastal Structure of the Continental Margin, Northwest Peru and
Southwest Equador.
Memoir Geological Society of America, Vol.154.
20. Spector, A. and Grant F. S. (1970)
Statistical Models for Interpreting Aeromagnetic Data.
Geophysics, Vol.35-2, p.293-302.
21. Talwani, M et al (1959)
Rapid Gravity Computations for Two-Dimensional Bodies with Application
to the Mendocino Submarine Fracture Zone.
JGR, Vol.64-1, p.49-59.
22. Welson, J. (1984)
Geologia de los cuadrangulos de Jayanca, Incahuasi, Cutervo, Chiclayo,
Chongoyape, Chota, Celendin, Pacasmayo y Chepen.
INGEMMET, Serie A. Vol.38.

